Available online at www.sciencedirect.com
ScienceDirect
Cement and Concrete Research 37 (2007) 639 – 646
Cement and Concrete Research

Mineralogical phase analysis of alkali and sulfate bearing belite rich laboratory clinkers

Khadija Morsli [a,b], Ángeles G. de la Torre [a], Mohammed Zahir [b], Miguel A.G. Aranda [a,*]

[a] Departamento de Química Inorgánica, Cristalografía y Mineralogía, Universidad de Málaga, 29071 Málaga, Spain
[b] L.P.C.M. Département de Chimie, Faculté des Sciences, Université Chouaib Doukkali, El Jadida 24000, Morocco

Received 29 May 2006; accepted 26 January 2007

Abstract

The activation of laboratory belite clinkers has been carried out by adding variable amounts of alkaline salts (K_2CO_3, Na_2CO_3), and/or SO_3 as gypsum in the raw materials but keeping almost constant the main elements ratios, Ca/Si/Al/Fe. Quantitative phase analyses by the Rietveld method using high resolution synchrotron and strictly monochromatic CuKα_1 laboratory X-ray powder diffraction data has been performed. Quantitative phase analysis results have been compared to validate the protocol using laboratory X-ray data. The agreement in the results is noteworthy, which indicates that good quantitative phase analyses can be obtained from laboratory X-ray powder data. Qualitative studies have confirmed that the addition of alkaline salts to raw mixtures promotes the stabilization, at room temperature, of the highest temperature polymorphs: α'_H-C_2S and α-C_2S. Quantitative studies gave the phase assemblage for ten different laboratory belite clinkers. As an example, an active belite clinker with 1.0 wt.% of K_2O and 1.0 wt.% of Na_2O (amounts added to the raw mixtures) contains 8.5(3) wt.% of β-C_2S, 21.2 (3) wt.% of α'_H-C_2S, 24.1(2) wt.% of α-C_2S, 18.9(3) wt.% of total C_3S, 17.3(2) wt.% of C_3A and 10.0(2) wt.% of C_4AF. A belite clinker with 0.8 wt.% SO_3 (nominal loading) contains 60.7(1) wt.% of β-C_2S, 6.7(2) wt.% of α'_H-C_2S, 12.3(7) wt.% of C_3S, 9.1(2) wt.% of C_3A and 11.2 (2) wt.% of C_4AF. Overall, quantitative phase analyses have shown that alkaline oxides stabilize α'_H-C_2S and α-C_2S, sulfur stabilizes β-C_2S, with a large unit cell volume, and the joint presence of alkaline oxides and sulfur promotes mainly the stabilization of the α'_H-C_2S polymorph.

Keywords: Activated cements; X-ray diffraction; Characterization

1. Introduction

Cement industry requires vast amounts of energy to operate, especially to burn cement clinker and to grind raw and produced materials. This power consumption leads to a concomitant release of CO_2 into atmosphere, up to 0.97 tons of CO_2 per ton of Ordinary Portland cement (OPC) produced. Considering these values, cement industry contributes around 6% of all CO_2 anthropogenic emissions [1,2].

Belite Portland cements (BPCs) contain more than 50 wt.% of Ca_2SiO_4, belite, as the main mineralogical component, while Ca_3SiO_5, alite, is the most important phase in OPCs. The increasing interest of BPCs and related systems is mainly due to a lower CaO consumption and therefore the depletion of CO_2 emissions produced in the manufacturing process [3–5]. BPCs can be produced at a clinkerization temperature approximately 100 °C lower than that for OPC, which reduces CO_2 emissions from fuel burning [6]. BPCs based concretes are considered to be "low heat" ones and more durable than those derived from OPC. These performances make BPCs suitable to the construction of large dams and to the lining of oil wells. However, the massive application of these materials requires overcoming some drawbacks such as the low hydration rate of the belite phase and high resistance to be milled [2,7].

Cement nomenclature will be adopted hereafter, C=CaO, S=SiO_2, A=Al_2O_3, F=Fe_2O_3 and $\overline{S}$=SO_3, for simplifying the description of cement phases. Stoichiometric C_2S presents five polymorphs on heating, γ, β, α'_L, α'_H and α. One kind of activation of BPCs consists on the stabilization at room temperature of the high temperature polymorphs (i.e. α-forms), which are more reactive than β-C_2S [8]. The latter is the polymorph that commonly prevails in OPCs but due to its slow hydration kinetic they develop very little mechanical strength at

---

[*] Corresponding author. Tel.: +34 952131874; fax: +34 952132000.
E-mail address: g_aranda@uma.es (M.A.G. Aranda).

0008-8846/$ - see front matter © 2007 Elsevier Ltd. All rights reserved.
doi:10.1016/j.cemconres.2007.01.012

Table 1
Elemental composition of raw mixtures prepared to obtain the different belite clinkers, expressed as oxide in wt.%

	CaO	SiO_2	Al_2O_3	Fe_2O_3	SO_3	K_2O	Na_2O	MgO	TiO_2	SrO	P_2O_5
B_ref	62.81	25.00	6.34	5.23	0.01	0.27	0.13	0.07	0.01	0.09	0.04
B_05NK	62.43	24.85	6.30	5.20	0.01	**0.50**	**0.50**	0.07	0.01	0.09	0.04
B_10NK	61.80	24.60	6.24	5.14	0.01	**1.00**	**1.00**	0.07	0.01	0.09	0.04
B_08S	62.72	24.74	6.27	5.17	**0.81**	0.08	0.12	0.00	0.00	0.09	0.00
B_10S05N	62.21	24.48	6.21	5.12	**1.01**	0.26	**0.50**	0.07	0.01	0.09	0.04
B_10S15N	61.61	24.23	6.14	5.07	**1.01**	0.26	**1.50**	0.06	0.01	0.08	0.03
B_10S10K	62.01	24.39	6.18	5.10	**1.01**	**1.00**	0.12	0.06	0.01	0.08	0.04
B_10S20K	61.38	24.14	6.12	5.05	**1.01**	**2.00**	0.12	0.06	0.01	0.08	0.03
B_10S05NK	62.12	24.39	6.18	5.10	**1.01**	**0.50**	**0.50**	0.06	0.01	0.09	0.04
B_10S10NK	61.44	24.19	6.13	5.05	**1.01**	**1.00**	**1.00**	0.06	0.01	0.08	0.03

In bold the amount of nominal percentages of activator added is given.

early ages. The activation may be carried out by conventional firing using minor elements (dopants) such as alkalies, sulfur or barium additions [3] or by specific thermal treatments [9,10]. The stabilization of α-forms using alkalies was reported in previous studies [11]. The presence of an increasing amount of alkaline oxides in the BPCs (active-BPCs) yielded higher compressive strengths after 28 days when compared with alkali-free BPCs. Furthermore, sulfur is also commonly present in clinkers, mainly coming from fuels. This element is mainly dissolved in the melt that appears in the clinkerization process and it has a positive effect on the burnability of the raw mix [12]. On the other hand, sulfur also leads to a lattice modification of β-C_2S with improved hydraulic properties and it has been reported that the stabilization of α-forms cannot be achieved by this element [13]. In addition to that, SO_3 produces the shrinkage and the final disappearance of the C_3S primary phase volume in the quaternary phase diagram [14], $CaO–SiO_2–Al_2O_3–Fe_2O_3$. Although C_3S is a secondary phase in BPCs, its presence may be desirable as its hydration products lead to increase mechanical strength at early ages. Calcium sulfoaluminate cements are systems with high SO_3 contents and contain different amounts of $C_4A_3\overline{S}$, known as Klein's compound, which compensates belite low reactivity [7,15].

Final concrete performances depend on the mineralogical phase composition (and the texture properties). Quantitative phase analysis (QPA) of active-BPCs is very important and X-ray powder diffraction combined with the Rietveld method [16] is the most powerful tool to carry out this type of analysis. However, laboratory X-ray powder diffraction (LXRPD) data may contain systematic errors such as strong preferred orientation, optical aberrations that change with 2θ, microabsorption and strong peak overlapping of the different phases. High-Resolution Synchrotron X-ray Powder Diffraction (SXRPD) overcomes most of these drawbacks and it is often used to validate QPA obtained by LXRPD [17–21].

As part of our ongoing research about BPCs, laboratory clinkers with C_2S contents close to 60 wt.% were prepared and analyzed by QPA and LXRPD [22]. In that study, β-C_2S was the main polymorph due to absence of dopants. BPCs were activated [23] using Na_2O or K_2O and different amounts of high temperature C_2S polymorphs, α-forms, were quantified. The polymorph assignments were carried out by SXRPD data and selective dissolution of the clinkers to enrich the low content phases [23]. This work presents a continuation in the investigations of active BPCs. Here we show Rietveld QPA of clinkers activated with sulfur, with combinations of alkaline oxides and finally with sulfur and alkaline oxides. Ten BPCs have been analyzed using LXRPD data and also using SXRPD to validate the analyses of these complex materials. The influence of alkaline oxides and sulfur in the mineralogical phase assemblage is discussed.

2. Experimental section

2.1. Synthesis of belite-rich clinkers

Appropriated amounts of calcite (99% Aldrich), kaolin (Aldrich), quartz (99.59% ABCR) and iron oxide (99.95% AlfaAesar) were mixed in order to obtain a non-active belite clinker (B_ref) with theoretical mineralogical composition of 60 wt.% of C_2S, 16 wt.% of C_3S, 8 wt.% of C_3A and 16 wt.% C_4AF [22], according to Bogue's calculations [24]. Nine active belite clinkers have also been prepared by adding different amounts of Na_2O, K_2O and SO_3, to the raw mixture as Na_2CO_3 (99.999% Aldrich), K_2CO_3 (99% Aldrich) and gypsum ($CaSO_4·2H_2O$), respectively. The samples are labeled according to the amount of activator added, e. i., B_10S05NK stands for the active belite clinker with nominal composition of 1.0 wt.% of SO_3, 0.5 wt.% of Na_2O and 0.5 wt.% of K_2O. Table 1 gives

Table 2
Final S, K and Na contents in laboratory active belite clinkers

	SO_3	K_2O	Na_2O
B_ref	–	0.04/*0.27*	0.16/*0.13*
B_05NK	–	0.18/*0.50*	0.54/*0.50*
B_10NK	–	0.38/*1.00*	1.27/*1.00*
B_08S	0.71/*0.81*	0.06/*0.08*	0.20/*0.12*
B_10S05N	0.85/*1.01*	0.19/*0.26*	0.64/*0.50*
B_10S15N	0.79/*1.01*	0.19/*0.26*	1.28/*1.50*
B_10S10K	0.87/*1.01*	0.67/*1.00*	0.23/*0.12*
B_10S20K	0.79/*1.01*	1.10/*2.00*	0.25/*0.12*
B_10S05NK	0.96/*1.01*	0.33/*0.50*	0.53/*0.50*
B_10S10NK	0.88/*1.01*	0.58/*1.00*	1.06/*1.00*

Results are expressed as oxides in wt.%. The initial contents are also given in italics.

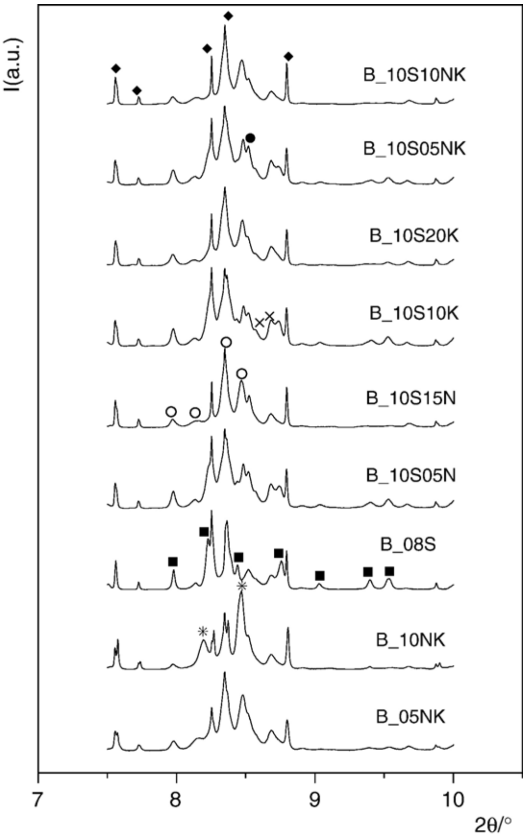

Fig. 1. Selected range of X-ray synchrotron powder diffraction raw data ($\lambda = 0.40$ Å) for all active belite clinkers. Some peaks mainly due to a given phase are labeled: β-C_2S ■; α'_H-C_2S ○; α-C_2S ✳; C_3S ◆; C_3A ●; and C_4AF ×.

the nominal dosages, expressed as oxide, used to prepare all the clinkers. Raw materials were mixed in an agate mortar with the aid of ethanol and dried in a stove at 60 °C. This treatment was performed three times. The clinkerization was carried out by pressing the raw mixtures into pellets of ~1.8 g with ~16 mm of diameter. The pellets were placed on Pt/Au crucibles and heated at 5 °C/min to 900 °C, which was held for 30 min. The temperature was then raised at a rate of 5 °C/min up to 1365 °C and held for 15 min. Finally, the clinkers were cooled from the highest temperature applying air flow (approximate rate cooling of 2000 °C/min).

2.2. Chemical analysis

The elemental composition of calcite was determined by X-ray fluorescence spectroscopy on Phillips PW-1404 spectrophotometer. The elemental composition of kaolin was measured by inductively coupled plasma atomic emission spectroscopy (ICP-AES) on an IRIS Advantage instrument from Thermo Jarrel Ash. SiO_2 (quartz—99.5% from ABCR), Fe_2O_3 (99.95% from Alfa Aesar), Na_2CO_3 (99.99% from Aldrich), K_2CO_3 (99%+ from Aldrich) and gypsum were used as purchased. The final Na and K contents in clinkers were determined by atomic emission spectroscopy in a Perkin-Elmer AAnalyst 800. The final sulfate content was measured by gravimetric method in accordance with EN 196-2.

2.3. X-ray powder diffraction

All the clinkers were finely ground to perform powder diffraction measurements. SXRPD patterns were collected on ID31 diffractometer of European Synchrotron Radiation Facility, (Grenoble, France) in Debye–Scherrer (transmission) configuration. The wavelength, $\lambda = 0.40084(5)$ Å (30.94 keV), was selected with a double-crystal Si (111) monochromator and calibrated with Si NIST ($a = 5.431195$ Å). Samples were loaded in borosilicate glass capillaries of diameter of 1.5 mm and rotated during data collection. The data acquisition time was ~45 min to have very good statistics over the angular range 3–30° (in 2θ). The data from the multi-analyzer Si(111) stage coupled with the scintillation detectors were normalized and summed up to 0.003° step size with local software to produce the final raw data.

LXRPD data have been recorded with an X'Pert MPD PRO diffractometer (PANalytical) using CuKα_1 radiation ($\lambda = 1.54059$ Å), [Ge(111) primary monochromator]. The optics configuration was a fixed divergence slit (1/2°), a fixed incident antiscatter slit (1°), a fixed diffracted anti-scatter slit (1/2°) and an X'Celerator RTMS (Real Time Multiple Strip) detector, working in scanning mode with maximum active length. The data were collected from 10° to 70° (2θ) during ~2 h. The samples were rotated during data collection at 16 rpm in order to enhance particle statistics. The X-ray tube worked at 45 kV and 35 mA.

Powder diffraction patterns were analyzed by the Rietveld method with GSAS software package [25] by using a pseudo-Voigt peak shape function [26] with the asymmetry correction included [27]. The refined overall parameters were: background coefficients, cell parameters, zero-shift error, peak shape parameters and phase fractions. Some phases present anisotropic line shape broadening, which was modeled using the phenomenological multi-dimensional distribution of lattice metrics approach [28] for SXRPD patterns and the ellipsoidal broadening correction for LXRPD patterns. The spherical-harmonic correction [29] was applied when needed in LXRPD patterns to correct texture problems for C_3S phase.

2.4. Scanning electron microscopy

Small pieces of pellets of some clinkers were mounted in epoxy resins and were progressively diamond polished down to 3 μm. Finally, a mechanical etching with 0.3 μm alumina paste was applied in order to create contrast among different phases. A Field Emission Scanning Electron Microscope (FESEM) (Hitachi-S4700) was used to perform the microstructure study.

3. Results and discussion

3.1. Chemical analysis

Some methodologies for the activation of BPCs require the dosage to the raw mixtures of compounds in part volatiles. This provokes a concern of the extent of that liberation during the heating process. To address that issue, Na, K and S contents

Table 3
Rietveld quantitative phase analysis results of all the clinkers in wt.% obtained from SXRPD data (upper values) and from LXRPD data (italics)

w	α-C_2S	α′$_H$-C_2S	β-C_2S	C_3S_T	C_3S_{M3}	C_3A_{CII}	C_3A_{ort}	C_4AF	C_4AF-I	K_2SO_4	$K_3Na(SO_4)_2$
B_ref	–	18.5(2)	46.7(1)	9.3(2)	3.9(2)	10.1(1)	–	11.5(1)	–	–	
	–	*15.5(3)*	*51.2(2)*	*9.6(1)*	*3.70(6)*	*8.9(2)*	–	*11.1(2)*	–	–	–
B_05NK	8.8(1)	32.3(2)	19.2(2)	7.8(3)	8.1(3)	6.6(2)	5.7(2)	8.4(1)	3.1(1)	–	–
	8.5(2)	*31.7(3)*	*22.7(4)*	*7.3(7)*	*8.8(7)*	*5.2(3)*	*4.9(3)*	*10.9(2)*	–	–	–
B_10NK	24.1(2)	21.2(3)	8.5(3)	6.2(3)	12.7(3)	–	17.3(2)	6.2(2)	3.8(2)	–	–
	27.3(3)	*19.3(4)*	*10.5(5)*	*8.6(4)*	*10.5(5)*	–	*14.7(4)*	*9.1(3)*	–	–	–
B_08S	–	6.7(2)	60.74(8)	12.26(7)	–	9.1(1)	–	8.4(1)	2.8(1)	–	–
	–	*5.8(4)*	*61.3(2)*	*12.8(1)*	–	*9.7(2)*	–	*10.4(2)*	–	–	–
B_10S05N	–	28.0(1)	39.9(1)	11.36(7)	–	9.72(9)	–	8.92(9)	2.10(8)	–	
	–	*24.9(3)*	*46.8(3)*	*9.8(2)*	–	*9.5(2)*	–	*9.0(2)*	–	–	–
B_10S15N	5.0(1)	42.0(2)	12.2(3)	17.00(8)	–	–	13.5(1)	8.1(2)	2.2(1)	–	–
	1.7(2)	*52.1(3)*	*12.0(5)*	*16.3(2)*	–	–	*10.8(3)*	*7.1(2)*	–	–	–
B_10S10K	–	23.9(1)	41.7(1)	12.72(7)	–	9.0(1)	–	9.4(1)	2.47(8)	0.29(3)	0.52(4)
	–	*20.1(3)*	*47.3(3)*	*12.3(2)*	–	*8.9(2)*	–	*10.4(2)*	–	*0.62(9)*	*0.38(7)*
B_10S20K	–	37.7(2)	23.5(2)	15.37(8)	–	8.8(1)	2.1(1)	8.9(1)	2.7(1)	0.93(4)	–
	–	*39.2(3)*	*24.7(4)*	*15.7(2)*	–	*5.9(3)*	*3.2(3)*	*10.4(2)*	–	*0.9(1)*	–
B_10S05NK	–	32.1(1)	33.3(2)	12.79(7)	–	9.85(9)	–	9.04(9)	2.18(8)	–	0.74(4)
	–	*26.8(3)*	*39.9(3)*	*14.0(2)*	–	*8.4(2)*	–	*10.5(2)*	–	–	*0.40(1)*
B_10S10NK	4.8(1)	41.2(2)	11.8(3)	17.33(8)	–	1.6(1)	11.5(1)	8.0(1)	2.6(1)	–	1.17(6)
	2.4(3)	*46.3(3)*	*12.2(4)*	*18.2(2)*	–	*1.5(2)*	*9.0(4)*	*9.1(2)*	–	–	*1.3(2)*

have been measured in the final clinkers; see Table 2, where they are expressed as oxides. It can be seen that sodium mainly remains in the clinker with very little volatilization ratio in the used experimental conditions. It must be highlighted that there is a slight overestimation in sodium oxide contents in the final clinkers when compared to the nominal starting compositions, see Table 2. Na_2O content has been determined by two different techniques, ICP-AES for raw materials and atomic emission spectroscopy for the final clinkers. The different measuring techniques are likely the source of the disagreement in the measured sodium contents. Potassium volatilization extent can be as high as 50% and it is rather variable. On the other hand, sulfur volatilization amount is comparatively smaller ranging between 10–20%. However, it must be highlighted that element volatilization levels strongly depend on the heating experimental conditions including the ratio between gases and raw materials. Hence, further studies are needed to extrapolate these results to industrial applications.

3.2. Quantitative phase analysis using SXRPD data

High-belite clinkers are complex materials due to the presence of many crystalline phases. Furthermore, most of these components display polymorphism and active belite clinkers may have more phases than ordinary belite clinkers. In these conditions, the use of high resolution SXRPD data is important to obtain accurate QPA. However, SXRPD is expensive and it is mainly used to validate the quantitative results obtained from LXRPD analyses. Fig. 1 shows a selected range of SXRPD patterns of active belite clinkers where some peaks due to a given phase are labeled. Qualitatively, it can be observed that the addition of minor amounts of activators induces strong modifications in the powder patterns. Prior to the QPA, all crystalline phases were identified as previously reported [23]. Table 3 gives the mineralogical compositions for all synthesized belite clinkers obtained by Rietveld QPA of SXRPD data.

The first result to be emphasized is the absence in all the clinkers of free lime (CaO) and γ-C_2S. The absence of the first indicates that thermal treatment was appropriate. On the other hand, the quenching from high temperature has avoided the β → γ polymorphic transformation of C_2S. γ-C_2S is hydraulically inactive and its presence is undesirable in BPCs.

In all laboratory belite clinkers β-C_2S [30] was present. The stabilization of this phase is due to both the rapid cooling rate and the presence of foreign ions into its structure. The addition of alkaline cations and sulfur to the raw mixture has also promoted α′$_H$-C_2S [31] stabilization in all belite clinkers, Table 3. It has to be noticed that increasing contents of K_2O and/or Na_2O, for a fixed SO_3 content, favor α′$_H$-C_2S stabilization, with the concomitant decrease of β-C_2S percentage. This preferential incorporation of alkaline cations into dicalcium silicate phases

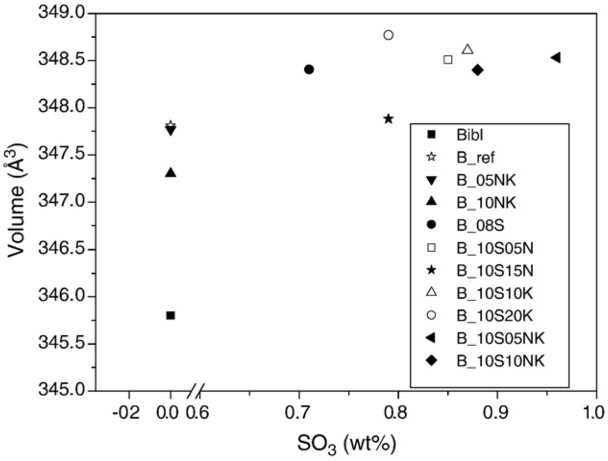

Fig. 2. Variation of β-C_2S unit cell volumes as a function of SO_3 wt.% content of the clinkers. The volume for stoichiometric β-C_2S was taken from [30].

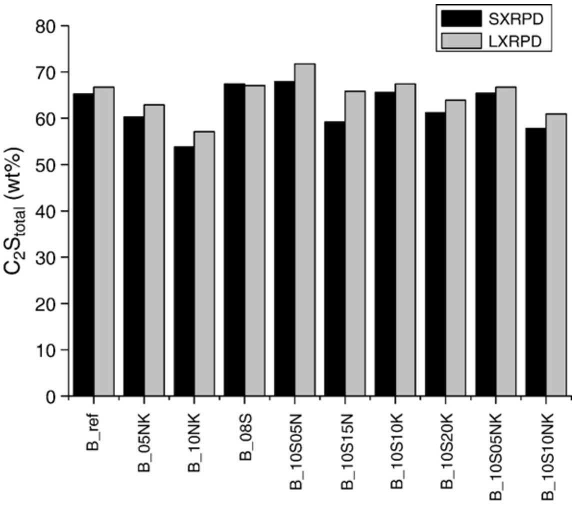

Fig. 3. Comparison of the quantitative phase analysis of total C_2S using synchrotron and laboratory X-ray diffraction data.

was previously reported [11], although quantitative phase analyses were not reported. High alkali-bearing belite clinkers (B_05NK, B_10NK, B_10S15N and B_10S10NK) also contain different amounts of α-C_2S [30], Table 3. The stabilization of the highest temperature C_2S polymorphs due to alkaline oxides has been reported in a previous work [23] using selective dissolution methodology and SXRPD. It is known that the role of K_2O and Na_2O in phase stabilization is not the same. Na_2O, in the presence of sulfur, promotes higher amounts of α'_H-C_2S and C_3S than K_2O does, see Table 3. The formation of alkaline sulfates strongly depends on the manufacturing process. In this study, belite clinkers have been prepared in a static electric furnace, thus the amount of minor phases, i.e. K_2SO_4 and/or $K_3Na(SO_4)_2$ is small, see Table 3. At an industrial stage, the stabilization of sulfate phases may be more important due to the gases and raw materials ratio.

It was reported [13] that the stabilization of α-forms of C_2S could not be achieved by SO_3 contents up to 1.5 wt.%. In this work, the stabilization of 6.7(2) wt.% of α'_H-C_2S has been accomplished only with 0.71 wt.% of SO_3 in B_08S, see Table 2, although α-C_2S is not present in that sample, see Table 3. β-C_2S rate of hydration is slower than those of C_3S and α-forms. However, a lattice-disturbed doped β-C_2S will improve hydraulic activity [32]. Fig. 2 shows the refined β-C_2S cell volume as a function of final SO_3 content. A slight expansion in the cell volume with increasing sulfur content can also be observed. β-C_2S of sulfur-free belite clinkers (B_ref, B_05NK and B_10NK) also present unit cell volume expansion due to their alkaline content, although the extension of this enlargement is smaller, see Fig. 2.

Belite clinkers synthesized in this work have the dosages to contain more than 15 wt.% of C_3S in order to provide relative rapid setting and early strength development. It is well known [14] that sulfur induces higher C_2S formation while C_3S content is decreased. B_08S and B_10S05N contain more than 65.0 wt.% of total C_2S, the highest ones, and the smallest amount of C_3S, see Table 3. These effects may produce a reduction in the compressive strengths at very early ages. On the other hand, active belite clinkers with high amounts of Na_2O, see Table 2, B_10NK, B_10S15N and B_10S10NK, contain more than 17.0 wt.% of C_3S, Table 3. The triclinic room temperature polymorph of C_3S [33] was used to model this phase in all the clinkers except for B_ref, B_05NK and B_10NK, in which a mixture of triclinic and monoclinic M_3 [34] was required to properly fit the patterns. The presence of sulfur avoids/minimizes the stabilization of M_3–C_3S [35], see Table 3.

Stoichiometric C_3A is cubic and does not present polymorphism. Nevertheless, the presence of foreign ions, especially Na^+, induces some structural modifications [36]. The pseudo-polymorph orthorhombic-C_3A [37] was only observed in belite clinkers with high amounts of retained alkaline oxides, see Table 2. In the remaining samples, cubic CII–C_3A [37] or a mixture of CII and orthorhombic C_3A was used to quantify calcium aluminate phases, see Table 3.

The iron rich perovskite phase, C_4AF, was quantified with the structural description reported by Colville and Géller [38]. C_4AF is a member of the solid solution series $Ca_2(Fe_{2-x}Al_x)O_5$, with $x=1$ and this phase was suitably fitted the Fe content at the octahedral site fixed to 75% and, therefore, the tetrahedral site was 75% occupied by Al. Another phase of this solid solution was detected in the SXRPD patterns for all active belite clinkers. This second phase was accounted for using an

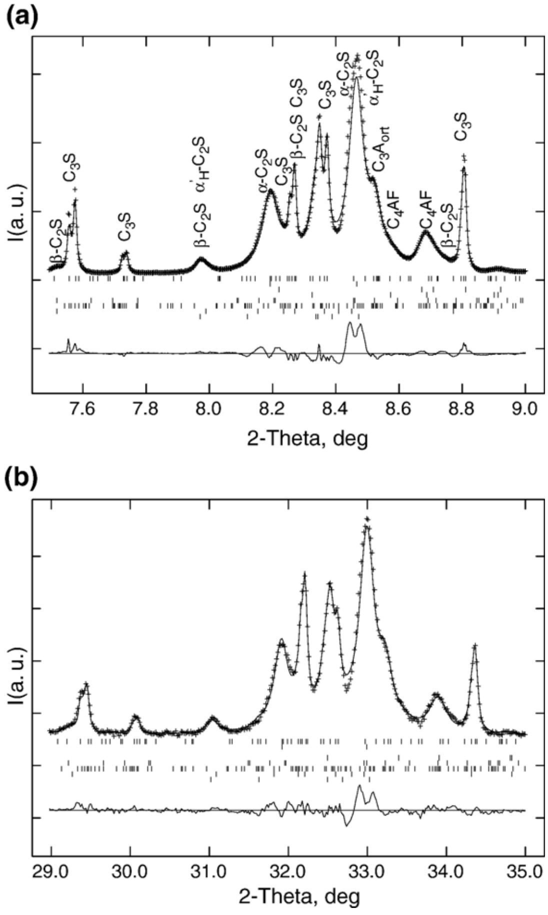

Fig. 4. Selected range of the Rietveld plots for B_10NK (a) SXRPD pattern and (b) LXRPD pattern. Peaks mainly due to a given phase have been labeled.

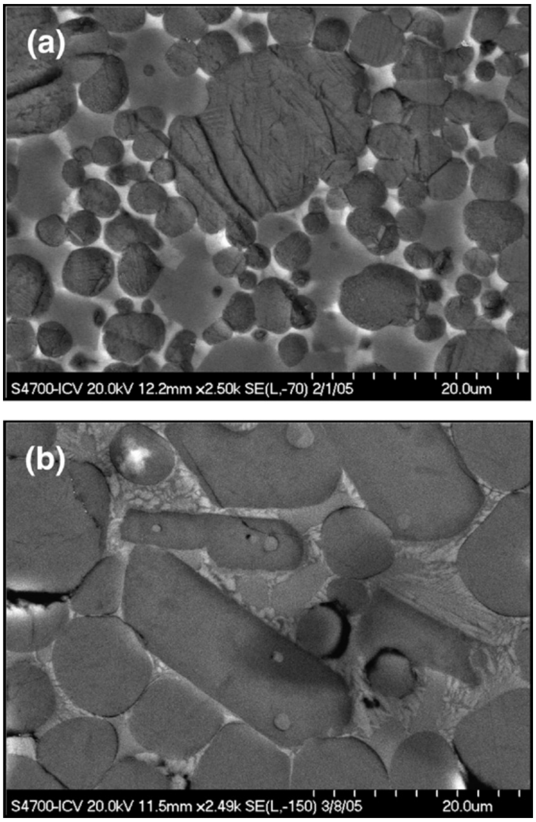

Fig. 5. SEM photographs of polished sections of (a) B_ref and (b) B_08S.

aluminum-rich member of the solid solution series [39], which has $x = 1.346$, and it will be labeled hereafter C_4AF-I.

3.3. *Comparison of quantitative phase analysis using SXRPD and LXRPD data*

Table 3 shows, in addition to QPA results using SXRPD patterns, the mineralogical composition for all belite clinkers obtained by analyzing LXRPD data. Overall, it has to be highlighted that synchrotron and laboratory X-ray results are in quite good agreement.

Total C_2S contents for all active belite clinkers obtained using both types of data are presented graphically in Fig. 3. It is noteworthy that this value is slightly overestimated using LXRPD data, Fig. 3, with the concomitant underestimation of C_3S, Table 3. This effect is very likely due to peak overlapping between these two phases. As an example to highlight this overlapping, Fig. 4 shows the same region of SXRPD and LXRPD Rietveld plots for B_10NK. As expected, the overlapping in the SXRPD pattern is smaller, which leads to more accurate QPA results. Furthermore, it is also evident in that figure that C_3S has narrow diffraction peaks, conversely, aluminates and C_2S forms have much broader peaks. These broader peaks are due to their microstructures with smaller microparticle sizes and more defects in those particles. It must be emphasized that all observed phases in the SXRPD were also observed in the LXRPD patterns excepting C_4AF-I, which was not computed in the LXRPD analyses.

In order to avoid deviations in the results, all sources of error during the refinements have to be carefully taken into account. For instance, β-C_2S and α'_H-C_2S present anisotropic peak broadening which was corrected using the phenomenological multi-dimensional distribution of lattice metrics approach [28] in SXRPD data analysis and with the ellipsoidal correction (STEC parameter of GSAS along [001]) in LXRPD refinements. Preferred orientation or texture effects are minimized in SXRPD data collection (rotating capillaries transmission geometry) but they have to be considered when analyzing LXRPD data (flat reflection geometry). This effect does not affect the quantification of belite phases but for C_3S it may become significant, especially in sulfur-bearing clinkers. Although C_3S content is slightly lower in sulfur-containing clinkers than in sulfur-free clinker, see Table 3, C_3S particle sizes are bigger in the former due to the predominance of crystal growth over nucleation [35]. To graphically show this, Fig. 5 gives SEM photographs for polished pieces of pellets of B_ref (a) and B_08S (b). Fig. 5(a) displays round particles of belite, with white zones where the liquid phases have crystallized, aluminates, and gray non-round particles are C_3S with sizes close to 10 μm. Fig. 5(b) also displays round particles of belite, but the sizes of the C_3S particles (almost perfect hexagonal

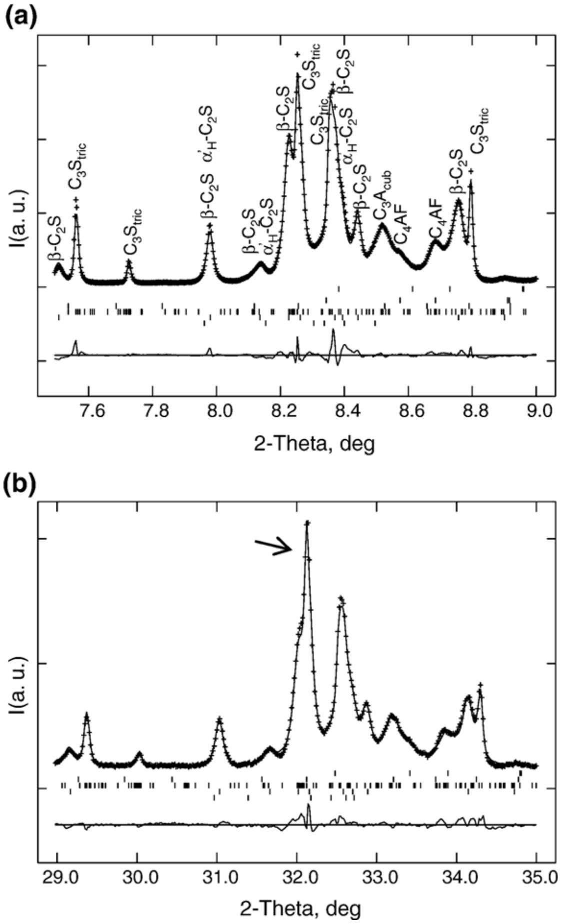

Fig. 6. Selected range of the Rietveld plots for B_08S (a) SXRPD pattern and (b) LXRPD pattern. Peaks mainly due to a given phase have been labeled. The arrow highlights C_3S texture effect in LXRPD pattern.

shape) are much larger, even bigger than 25 μm. Very large particles give easily texture effects in reflection geometry as shown in Fig. 6, which displays the same region of the SXRPD (a) and LXRPD (b) Rietveld plots for B_08S. The arrow in Fig. 6 highlights the texture effect in LXRPD Rietveld plot, which was corrected with the spherical harmonic correction [29] using order = 4. The texture index obtained was 1.3, a value of 1 for this parameter represents an ideal random powder whereas ∞ would stand for a single crystal. The SXRPD pattern for B_08S does not display preferred orientation as expected.

4. Conclusions

The activation of belite clinkers by stabilizing high temperature (α'_H and α) polymorphs of C_2S has been achieved by adding alkaline cations and/or sulfur. In addition to that, sulfur-bearing clinkers contain β-C_2S with bigger unit cell volumes. The presence of alkaline oxides, Na and K, led to large amounts of α-C_2S in some cases larger than 25 wt.%. The joint existence of alkaline oxides and SO_3 promotes large quantities of α'_H-C_2S, but the presence of SO_3 inhibits the crystallization of α-C_2S. Overall, Rietveld QPA from laboratory X-ray powder diffraction data gave good results, as they are similar to those obtained from high-resolution synchrotron X-ray transmission data.

Acknowledgments

The authors acknowledge Prof. S. de Aza, Dra. P. Pena and Dr. A. H. de Aza for their help in the polishing process and with scanning electron microscopy measurements. ESRF (Grenoble, France) is thanked for providing synchrotron beam time on ID31. K. Morsli thanks a studentship from AECI (Spain). Financial support from JA (Spain) FQM-113 grant is acknowledged.

References

[1] R. McCaffrey, Climate change and the cement industry, global cement and lime magazine, Environmental Special Issue, 2002, pp. 15–19.

[2] E. Gartner, Industrially interesting approaches to "low-CO_2" cements, Cem. Concr. Res. 34 (9) (2004) 1489–1498.

[3] A.K. Chatterjee, High belite cements. Present status and future technological options: part I, Cem. Concr. Res. 26 (8) (1996) 1213–1225.

[4] P.K. Mehta, Investigation on energy-saving cements, World Cem. Technol. 11 (5) (1980) 166–177.

[5] A.K. Chatterjee, Special cements, in: J. Bensted, P. Barnes (Eds.), Structure and Performance of Cements, Spon Spress, London, 2002, pp. 186–236.

[6] J. Stark, A. Muller, R. Seydel, K. Jost, Conditions of the existence of hydraulically active belite cement, Proceedings of the 8th International Congress of Cement Chemistry, Rio de Janeiro, vol. II, 1986, pp. 306–309.

[7] C.D. Popescu, M. Muntean, J.H. Sharp, Industrial trial production of low energy belite cement, Cem. Concr. Compos. 25 (7) (2003) 689–693.

[8] E.M. Gartner, Hydration of Portland cement, in: J. Bensted, P. Barnes (Eds.), Structure and Performance of Cements, Spon Spress, London, 2002, pp. 78–81.

[9] A.K. Chatterjee, Future technological options: Part, Cem. Concr. Res. 26 (8) (1996) 1227–1237.

[10] K. Fukuda, S. Ito, Improvement in reactivity and grindability of belite-rich cement by remelting reaction, J. Am. Ceram. Soc. 82 (8) (1999) 2177–2180.

[11] A. Gies, D. Knofel, Influence of alkalies on the composition of belite-rich cement clinkers and the technological properties of the resulting cements, Cem. Concr. Res. 16 (3) (1986) 411–422.

[12] K.G. Kolovos, S. Tsivilis, G. Kakali, Study of clinker dopped with P and S compounds, J. Therm. Anal. Calorim. 77 (2004) 759–766.

[13] A. Gies, D. Knofel, Influence of sulfur on the composition of belite-rich cement clinkers and the technological properties of the resulting cements, Cem. Concr. Res. 17 (2) (1987) 317–328.

[14] S. Uda, E. Asakura, M. Nagashima, Influence of SO_3 on the phase relationship in the system CaO–SiO_2–Al_2O_3–Fe_2O_3, J. Am. Ceram. Soc. 81 (3) (1998) 725–729.

[15] I. Odler, H. Zhang, Investigations on high SO_3, Portland clinkers and cements I. Clinker synthesis and cement preparation, Cem. Concr. Res. 26 (9) (1996) 1307–1313.

[16] H.M. Rietveld, A profile refinement method for nuclear and magnetic structures, J. Appl. Crystallogr. 2 (2) (1969) 65–71.

[17] P.M. Suherman, A.V. Riessen, B. Oconnor, D. Li, D. Bolton, H. Fairhurst, Determination of amorphous phase levels in Porltand cement clinker, Powder Diffr. 17 (2002) 178–185.

[18] V.K. Peterson, B.A. Hunter, A. Ray, L.P. Aldridge, Rietveld refinement of neutron, synchrotron and combined powder diffraction data of cement clinker, Appl. Phys., A 74 (2002) S1409–S1411.

[19] A.G. de la Torre, M.A.G. Aranda, Accuracy in Rietveld quantitative phase analysis of Portland cements, J. Appl. Crystallogr. 36 (5) (2003) 1169–1176.

[20] A. Emanuelson, A.R. Landa-Cánovas, S. Hansen, A comparative study of ordinary and mineralised Portland cement clinker from two different production units, Part II: characteristics of the calcium silicates, Cem. Concr. Res. 33 (2003) 1623–1630.

[21] V.K. Peterson, A. Ray, B.A. Hunter, A comparative study of Rietveld phase analysis of cement clinker using neutron, laboratory X-ray and synchrotron data, Powder Diffr. 21 (1) (2006) 12–18.

[22] A.G. de la Torre, M.A.G. Aranda, A.H. de Aza, P. Pena, S. de Aza, Belite Portland clinker. Synthesis and mineralogical analysis, Bol. Soc. Esp. Ceram. Vidr. 44 (3) (2005) 185–191.

[23] K. Morsli, A.G. de la Torre, S. Stöber, A.J.M. Cuberos, M. Zahir, M.A.G. Aranda, Quantitative Phase Analysis of Laboratory Active Belite Clinkers by Synchrotron Powder Diffraction, J. Amer. Ceram. Soc., (Submitted for publication).

[24] R.H. Bogue, Calculation of the compounds in Portland cement, Ind. Eng. Chem., Anal. Ed. 1 (4) (1929) 192–197.

[25] A.C. Larson, R.B. Von Dreele, General Structure Analysis System (GSAS), Los Alamos National Laboratory Report LAUR, vol. 86–748, 2000.

[26] P. Thompson, D.E. Cox, J.B. Hasting, Rietveld refinement of Debye–Scherrer synchrotron X-ray data from Al_2O_3, J. Appl. Crystallogr. 20 (2) (1987) 79–83.

[27] L.W. Finger, D.E. Cox, A.P. Jephcoat, A correction for powder diffraction peak asymmetry due to diaxial divergence, J. Appl. Crystallogr. 27 (1994) 892–900.

[28] P.W. Stephens, Phenomenological model of anisotropic peak broadening in powder diffraction, J. Appl. Crystallogr. 32 (1999) 281–289.

[29] R.B. Von Dreele, Quantitative texture analysis by Rietveld refinement, J. Appl. Crystallogr. 30 (1997) 517–525.

[30] W.G. Mumme, R.J. Hill, G. Bushnell-Wye, E.R. Segnit, Rietveld structure refinement, crystal chemistry and calculated powder diffraction data for the polymorphs of dicalcium silicate and related phases, Neues Jahrb. Mineral. Abh. 169 (1) (1995) 35–68.

[31] W.G. Mumme, L. Cranswick, B. Chakoumakos, Rietveld crystal structure refinements from high temperature neutron powder diffraction data for the polymorphs of dicalcium silicate, Neues Jahrb. Mineral. Abh. 170 (2) (1996) 171–188.

[32] J.F. Young, H.S. Tong, Microstructure and strength development of beta-dicalcium silicate pastes with and without admixtures, Cem. Concr. Res. 7 (1977) 627–636.

[33] N.I. Golovastikov, R.G. Matveeva, N.V. Belov, Crystal structure of the tricalcium silicate $3CaO \cdot SiO_2 = C_3S$, Sov. Phys. Crystallogr. 20 (4) (1975) 441–445.

[34] A.G. de la Torre, S. Bruque, J. Campo, M.A.G. Aranda, The superstructure of C_3S from synchrotron and neutron powder diffraction and its role in quantitative phase analyses, Cem. Concr. Res. 32 (9) (2002) 1347–1356.

[35] I. Maki, K. Fukuda, H. Yoshida, J. Kumaki, Effect of MgO and SO_3 on the impurity concentration in alite in Portland cement clinker, J. Am. Ceram. Soc. 75 (11) (1992) 3163–3165.

[36] H.F.W. Taylor, Cement Chemistry, Thomas Telford Ltd, London, 1997.

[37] Y. Takeuchi, F. Nishi, I. Maki, Crystal-chemical characterization of the $3CaO \cdot Al_2O_3–Na_2O$ solid-solution series, Z. Kristallogr. 152 (3–4) (1980) 259–307.

[38] A.A. Colville, S. Géller, The crystal structure of brownmillerite, Ca_2FeAlO_5, Acta Crystallogr., B 27 (12) (1971) 2311–2315.

[39] G.J. Redhammer, G. Tippelt, G. Roth, G. Amthauer, Structural variations in the brownmillerite series $Ca_2(Fe_{2-x}Al_x)O_5$ single-crystal X-ray diffraction at 25 °C and high-temperature X-ray powder diffraction ($25\,°C < T < 1000\,°C$), Am. Mineral. 89 (2004) 405–420.